

## Oxygen intercalation in mixed valence copper oxides related to the perovskites

by

Claude MICHEL and Bernard RAVEAU

Équipe Oxydes du Laboratoire de Cristallographie,  
Chimie et Physique des Solides, L. A. 251, ISMRa,  
Université, 14032 Caen Cedex, France.

**ABSTRACT.** — Intercalation of oxygen in ternary copper oxides has been studied for three series of compounds:  $\text{Ba}_3\text{La}_3\text{Cu}_6\text{O}_{14+\delta}$ ,  $\text{La}_{2-x}\text{A}_{1+x}\text{Cu}_2\text{O}_{6-x/2-\delta}$  and  $\text{La}_{2-x}\text{A}_x\text{CuO}_{4-x/2+\delta}$  ( $\text{A} = \text{Ca}, \text{Sr}, \text{Ba}$ ). These mixed valence copper oxides, characterized by the presence of  $\text{Cu(II)}$  and  $\text{Cu(III)}$  simultaneously are oxygen defect compounds whose structure is closely related to that of the perovskite, and to those of the two members of the intergrowths  $\text{SrO}$ -perovskite:  $\text{Sr}_3\text{Ti}_2\text{O}_7$  and  $\text{K}_2\text{NiF}_4$  respectively. The localization of the oxygen vacancies in  $(001)$  planes of these structures makes that two of these families:  $\text{Ba}_3\text{La}_3\text{Cu}_6\text{O}_{14+\delta}$  and  $\text{La}_{2-x}\text{A}_{1+x}\text{Cu}_2\text{O}_{6-x/2-\delta}$  can be considered in their most reduced state as oxides with low dimensionality. The influence of oxygen intercalation on the structure is described. The electrical properties of these phases are described and discussed: they are strongly influenced by the intercalation process. A progressive transition from a  $p$  type semi-conductive to a  $p$  type semi-metallic or metallic state is indeed observed which depends on the oxygen pressure and on the nature of the oxides.

**RÉSUMÉ.** — L'intercalation d'oxygène dans les oxydes ternaires de cuivre a été étudiée pour trois séries de composés :  $\text{Ba}_3\text{La}_3\text{Cu}_6\text{O}_{14+\delta}$ ,  $\text{La}_{2-x}\text{A}_{1+x}\text{Cu}_2\text{O}_{6-x/2+\delta}$  et  $\text{La}_{2-x}\text{A}_x\text{CuO}_{4-x/2+\delta}$  ( $\text{A} = \text{Ca}, \text{Sr}, \text{Ba}$ ). Ces oxydes de cuivre à valence mixte, caractérisés par la présence simultanée de  $\text{Cu(II)}$  et  $\text{Cu(III)}$ , sont des composés déficitaires en oxygène dont la structure est étroitement liée respectivement à celle de la pérovskite et à celles des deux membres de la série d'intercroissances pérovskite- $\text{SrO}$  :  $\text{Sr}_3\text{Ti}_2\text{O}_7$  et  $\text{K}_2\text{NiF}_4$ . La localisation des lacunes anioniques dans les plans  $(001)$  de ces structures fait que deux de ces familles :  $\text{Ba}_3\text{La}_3\text{Cu}_6\text{O}_{14+\delta}$  et  $\text{La}_{2-x}\text{A}_{1+x}\text{Cu}_2\text{O}_{6-x/2+\delta}$  peuvent être considérées, dans leur état le plus réduit, comme des oxydes de basse dimensionnalité. L'influence de l'intercalation d'oxygène dans la structure est décrite. Les propriétés électriques de ces phases sont décrites et discutées : elles sont fortement influencées par le processus d'intercalation. Une transition progressive d'un état semi-conducteur de type  $p$  à un état semi-métallique ou métallique de même type, qui dépend de la pression d'oxygène et de la nature des oxydes, est en effet observée.

## INTRODUCTION

Intercalation of oxygen in an oxide, by a simple reversible exchange with  $O_2$  in air or in a gaseous atmosphere can be used for different applications such as electrocatalysis, or gauges for materials with electrical properties sensitive to the oxygen content. Thus it appears that such oxides must exhibit rather large oxygen defects in their « reduced » form, and must be able to absorb oxygen from atmosphere tending towards a stoichiometric phase in their « oxidized » state. This phenomenon supposes a reversible change of the oxidation state and of the coordination number of the metallic atoms which participate to the framework of the oxide. In this respect, copper oxides are very good candidates, owing to the ability of copper to take several coordinations—octahedral, square pyramidal, square planar—and several oxidations stades: + 1, + 2, + 3. Cu(II) and Cu(III) must be especially considered owing to their possibility to take the same octahedral coordination in similar structures as shown from previous works on  $La_2Cu^{II}O_4$  [1-2] and  $LaSrCu^{III}O_4$  [3], which are isostructural with  $K_2NiF_4$ . Ternary oxides  $A_xCu_yO_3$  containing Cu(III) are more difficult to prepare than those with Cu(II), since oxygen pressures ranging from 1 bar [4-7] to several kbars [3-8] are most of the time necessary to synthesize these compounds. However, the presence of A elements like barium favours the formation of Cu(III) in normal pressure conditions [9-10]. The present paper deals with the soft intercalation of oxygen, *i. e.* at low pressure ( $p \leq 1$  atm) and at low temperature ( $T \sim 400-500^\circ C$ ) in three series of ternary copper oxides related to the perovskite [11-13] and belonging to the systems  $La_2O_3-AO-CuO$  with  $A = Ca, Sr, Ba$ . The influence of oxygen intercalation on the electron transport properties of these phases are discussed.

## STRUCTURAL CONSIDERATIONS

Three families with an oxygen defect structure have been isolated in the systems  $La_2O_3-AO-CuO$ :

- The oxygen defect perovskites  $La_3Ba_3Cu_6O_{14+\delta}$ .
- The oxygen defect intergrowths  $Sr_3Ti_2O_7$  type,  
 $La_{2-x}A_{1+x}Cu_2O_{6-x/2+\delta}$   $A = Ca, Sr$ .
- The oxygen defect intergrowth  $K_2NiF_4$  type,  $La_{2-x}A_xCuO_{4-x/2+\delta}$ .

The most reduced form which has been isolated for the defect perovskites  $La_3Ba_3Cu_6O_{14+\delta}$  corresponds to the formulation  $La_3Ba_3Cu_6O_{14}$ . Its

structure (fig. 1) can be described as an ordered oxygen defect perovskite. All the metallic sites corresponding to the stoichiometric perovskite are occupied by copper ions and lanthanum and barium ions respectively, whereas only 7/9 of the anionic sites are occupied in an ordered manner.

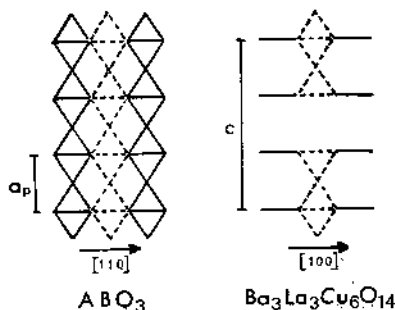


Fig. 1. — Schematic structure of a stoichiometric  $ABO_3$  perovskite and the defect oxygen perovskite  $Ba_3La_3Cu_6O_{14}$ .

Considering the tetragonal cell of this compound ( $a \simeq a_p\sqrt{2} = 5.525 \text{ \AA}$ ,  $c \simeq 3a_p = 11.721 \text{ \AA}$ ), it can indeed be seen that the basal planes of the octahedra, parallel to  $(001)$  are preserved, that one apex out of two is missing at the levels  $z = 1/6$  and  $5/6$ , whereas all the apices of these octahedra are missing at  $z = 1/2$ . It results that this reduced form can be considered as a true layer structure: double defect perovskite layers  $[Ba_{1.5}La_{0.5}Cu_3O_7]_2$  built up from corner-sharing, octahedra  $CuO_6$  square pyramids  $CuO_5$  and square groups  $CuO_4$  are observed whose cohesion is ensured by lanthanum ions located at  $z = 1/2$ . It is remarkable that such an oxide is characterized by a high Cu(III) content in spite of the high oxygen defect content. Site potential calculations confirm that the  $Cu^{3+}$  ions are located preferentially on the octahedral sites. It must also be noted that this limit compound has not really been synthesized. By heating in air at  $1000^\circ \text{C}$  for 24 h the mixture of  $La_2O_3$ ,  $CuO$  and  $BaCO_3$  and quenching the samples at room-temperature a slight excess of oxygen is indeed observed corresponding to the formulation  $La_3Ba_3Cu_6O_{14.10}$ . The most reduced phase  $La_3Ba_3Cu_6O_{14.05}$  is then synthesized by annealing the sample  $La_3Ba_3Cu_6O_{14.10}$  at  $400^\circ \text{C}$  under low oxygen pressure ( $\sim 5.10^{-3}$  bar) during several hours.

The deviation from stoichiometry in the oxides  $La_{2-x}A_{1+x}Cu_2O_{6-x/2+\delta}$  is more complex owing to the possibility of substitution of calcium or strontium for lanthanum, in a small homogeneity range ( $0 \leq x \leq 0.14$  for

strontium and  $x = 0.10$  for calcium). The most reduced oxide which has been isolated in this family corresponds to the formulation  $\text{La}_2\text{SrCu}_2\text{O}_6$ . Its tetragonal cell ( $a = 3.865 \text{ \AA}$ ,  $c = 19.887 \text{ \AA}$ ), corresponds to a structure closely related to that of  $\text{Sr}_3\text{Ti}_2\text{O}_7$  (fig. 2 a).  $\text{Cu}^{2+}$  ions are indeed located on the  $\text{Ti}^{4+}$  sites,  $\text{La}^{3+}$  and  $\text{Sr}^{2+}$  ions are located on the  $\text{Sr}^{2+}$  sites, whereas six anionic sites out of seven are occupied by oxygen in an ordered manner; thus, this oxide can be considered as an intergrowth of double oxygen perovskite layers and SrO type layers. The perovskite layers exhibit some similarity with those observed for  $\text{La}_3\text{Ba}_3\text{Cu}_6\text{O}_{14}$ : the basal planes of the octahedra parallel to (001) are also preserved whereas at  $z = 0$  and  $z = 1/2$  all the apices of the oxygen octahedra are missing. However, the resulting configuration of the framework is different from  $\text{La}_3\text{Ba}_3\text{Cu}_6\text{O}_{14}$ :  $\text{Cu(II)}$  exhibits here only one coordination which is square pyramidal. Nevertheless this oxide, like  $\text{La}_3\text{Ba}_3\text{Cu}_6\text{O}_{14}$ , must be considered as a structure with low dimensionality. It can indeed be described as built up from slabs  $|\text{LaSrCu}_2\text{O}_6|_\infty$  parallel to (001) whose cohesion is ensured by  $\text{Sr}^{2+}$  and  $\text{La}^{3+}$  ions located at  $z = 0$  and  $z = 1/2$ . The  $|\text{LaSrCu}_2\text{O}_6|_\infty$  slabs are themselves an intergrowth of SrO-type layers and corner-sharing square pyramid layers. Such slabs are in fact derived from the  $\text{K}_2\text{NiF}_4$  structure: the latter corresponds indeed to the superposition of two  $|\text{K}_2\text{Ni}_2\text{F}_6|_\infty$  slabs which would share the face of their square pyramids, forming  $\text{NiF}_6$  octahedra (fig. 2 b). Like  $\text{La}_3\text{Ba}_3\text{Cu}_6\text{O}_{14+\delta}$ ,  $\text{La}_2\text{SrCu}_2\text{O}_6$  is

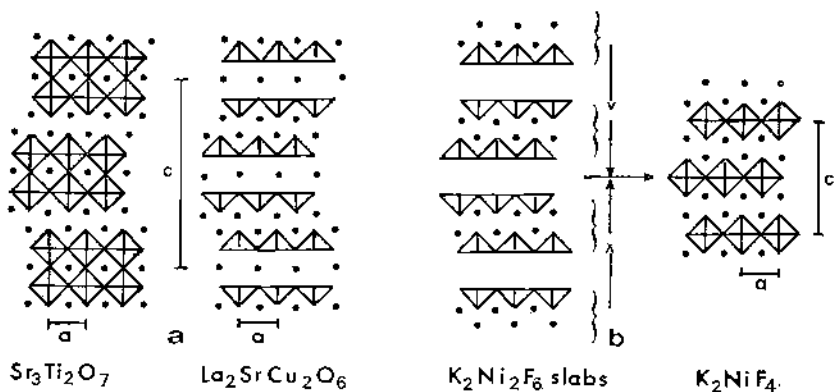


Fig. 2.

- a) Schematic structure of  $\text{Sr}_3\text{Ti}_2\text{O}_7$  and  $\text{La}_2\text{SrCu}_2\text{O}_6$  (projection on to (100) plane), showing the oxygen vacancies.
- b) Schematic representation of  $\text{K}_2\text{Ni}_2\text{F}_6$  slabs sharing the square faces of the  $\text{NiF}_5$  pyramids to give the  $\text{K}_2\text{NiF}_4$  structure.

characterized by a great stability in spite of its oxygen defect structure: it is indeed synthesized by heating the stoichiometric mixture of  $\text{CuO}$ ,  $\text{La}_2\text{O}_3$  and  $\text{SrCO}_3$  at 1 050-1 100° for 24 h in air and by quenching them at room temperature in order to avoid their oxidation at lower temperature. Contrary to  $\text{La}_3\text{Ba}_3\text{Cu}_6\text{O}_{14}$ , copper is in its lower oxidation state,  $\text{Cu(II)}$  in this oxide.

The oxides  $\text{La}_{2-x}\text{A}_x\text{CuO}_{4-x/2+\delta}$  exhibit an oxygen defect  $\text{K}_2\text{NiF}_4$  type structure involving different coordinations of copper: octahedral, square pyramidal and eventually square planar (fig. 3). Their oxygen content

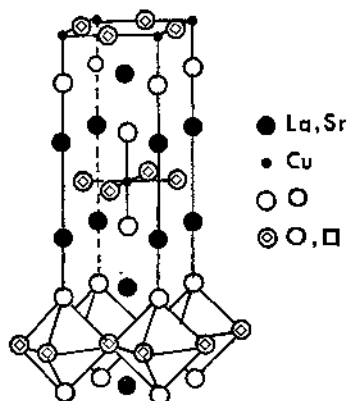


Fig. 3. — Perspective view of the structure of the oxides  $\text{La}_{2-x}\text{Sr}_x\text{CuO}_{4-x/2+\delta}$  with oxygen vacancies located in the basal plane of the octahedra.

depends on the nature of the A ions ( $A = \text{Ca}, \text{Sr}, \text{Ba}$ ) and on the substitution rate  $x$  which can lead to wide homogeneity ranges:  $0 \leq x \leq 0.20$  for  $A = \text{Ca}$  and  $\text{Ba}$  and  $0 \leq x \leq 4/3$  for  $A = \text{Sr}$ . The most reduced phase which exhibits the highest deviation from stoichiometry has been synthesized in the case of strontium for  $x = 4/3$ :  $\text{La}_{2/3}\text{Sr}_{4/3}\text{CuO}_{3.33}$ . Contrary to the two other series, the oxygen vacancies are located in the basal plane of the octahedra which are parallel to the  $(001)$  plane of the tetragonal cell ( $a = 3.759 \text{ \AA}$ ,  $c = 12.907 \text{ \AA}$ ). It must also be emphasized that this type of localization of the oxygen vacancies is always observed whatever the nature of the A ions, and whatever the rate of substitution  $x$  may be. However, symmetry changes and order-disorder phenomena in this plane may appear according to the nature of A and  $x$  value (table I). So, the calcium and barium oxides are characterized by a monoclinic distortion of the tetragonal  $\text{K}_2\text{NiF}_4$  structure, whatever the  $x$  value may be  $0 \leq x \leq 0.20$ ; the same

is true for the strontium compounds with  $0 \leq x \leq 0.10$ . Thus, the oxides corresponding to these homogeneity ranges exhibit an orthorhombic cell related to that of  $K_2NiF_4$  in the following way:  $a \simeq b \simeq aK_2NiF_4 \sqrt{2}$  and  $c \simeq cK_2NiF_4$ .

TABLE I

*The oxides  $La_{1-x}A_xCuO_{4-x/2+\delta}$ : crystallographic data and analytical results (quenched materials).*

A	x	$\delta$	Cell parameters (Å)			Heating temperature °C
			a	b	c	
	0		5.366	5.402	13.149	1,100
Ba	0.05	0.01	5.361	5.380	13.201	1,100
	0.1	0.02	5.359	5.364	13.245	1,100
	0.2	0.05	5.356		13.320	1,100
Ca	0.05	0.01	5.351	5.387	13.150	1,100
	0.1	0.02	5.356	5.385	13.174	1,100
	0.2	0.05	5.357	5.380	13.210	1,100
Sr	0.08	0.03	5.351	5.368	13.200	1,000
	0.16	0.04	3.774		13.231	1,000
	0.25	0.07	3.775		13.247	1,000
	0.33	0.11	3.774		13.254	1,100
	0.50	0.10	3.776		13.210	1,160
	0.66	0.075	3.775		13.160	1,170
	0.88	0.06	3.769		13.070	1,170
	1.0	0.005	3.767 (*)		13.002	1,200
	1.20	0.0	5 × 3.76		12.940	1,200
	1.33	0.0	3.759 (*)		12.907	1,200

(\*) These a parameters are those of the tetragonal subcell.

On the other hand, the strontium compounds exhibit a tetragonal symmetry similar to that of  $K_2NiF_4$  or  $LaSrCuO_4$  [3] for  $0.10 < x < 1$  ( $a \simeq aK_2NiF_4$ ;  $c \simeq cK_2NiF_4$ ), whereas for  $1 \leq x \leq 4/3$ , superstructures appear on the electron diffraction patterns which involve tetragonal cells with  $a = b \simeq naK_2NiF_4$ ,  $n$  ranging from 1 to 6 according to the composition,  $c$  remaining unchanged ( $c \simeq cK_2NiF_4$ ). These oxides are very stable in spite of the high deviation from stoichiometry; for instance  $La_{2/3}Sr_{4/3}CuO_{3.33}$  is prepared by heating a mixture of the compounds  $La_2O_3$ ,  $CuO$  and  $SrCO_3$  at 1 200° C and quenching the phase at room temperature. It appears here that the most reduced phase exhibits also only Cu(II) like  $La_2SrCu_2O_6$  belonging to the second series. The oxides  $La_{2-x}A_xCuO_{4-x/2+\delta}$  appear very closely related to the second series formulated  $La_{2-x}A_{1+x}Cu_2O_{6-x/2+\delta}$  in that they can be considered as being respectively the members  $n = 1$  and 2 of a series of oxygen defect intergrowths between perovskite and

SrO structures, corresponding to the general formulation  $A_{n+1}B_nO_{3n+y}$ . However the behaviour of  $La_{2-x}A_xCuO_{4-x/2+\delta}$  is very different from the two other series in that it cannot be considered in its most reduced form as an oxide with low dimensionality.

### OXYGEN INTERCALATION AND DESINTERCALATION: INFLUENCE ON THE STRUCTURE

Oxygen can be intercalated in these three series of oxides by simple annealing of the materials at low temperature, *i. e.* 400° C-500° C, under different oxygen pressures.

The oxygen defect perovskite  $La_3Ba_3Cu_6O_{14.10}$  synthesized in air can absorb rather important oxygen amounts by annealing the samples at 400° C under oxygen pressures ranging from  $10^{-2}$  to 1 bar as shown from table II. In the same way, oxygen can be desintercalated from the structure of  $La_3Ba_3Cu_6O_{14.10}$  or from more oxidized compounds by simply annealing the samples always at 400° C under lower oxygen pressure,  $5.10^{-3}$  bar (table II). Thus it appears that the intercalated oxides  $La_3Ba_3Cu_6O_{14+\delta}$

TABLE II

*Evolution of  $\delta$  as a function of the oxygen pressure after annealing the oxide  $La_3Ba_3Cu_6O_{14.10}$  at 400° C.*

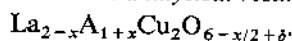
$PO_2$ (bar)	$5.10^{-3}$	$10^{-2}$	$2.10^{-1}$	$5.10^{-2}$	0.1	0.2	1
$\delta$	0.05	0.19	0.25	0.31	0.33	0.37	0.43

exhibit a rather wide homogeneity range  $0.05 \leq \delta \leq 0.43$ . The intercalation of oxygen in this structure does not influence the cell parameters, since the most oxidized compound,  $La_3Ba_3Cu_6O_{14.43}$ , is characterized by parameters very similar to those of  $La_3Ba_3Cu_6O_{14.10}$ ,  $a = 5.529 \text{ \AA}$  and  $c = 11.729 \text{ \AA}$ , whereas no parameter change with respect to the air synthesized oxide is observed when  $\delta$  tends towards zero. It is of course not possible to localize the additional oxygen in the structure by X ray diffraction; however site potential calculations [14], assuming that  $Cu^{3+}$  is octahedrally coordinated, show that this additional oxygen should be located between two square pyramids  $CuO_5$ , *i. e.* at  $z = 1/2$ , between the layers described above, forming corner-sharing ribbons of  $CuO_6$  octahedra running along  $\vec{c}$ . The electron transport properties of these compounds, which will be discussed further, are in agreement with this hypothesis. The fact that

the  $c$  parameter does not vary, in spite of the intercalation of rather great amounts of oxygen is easily explained by the high oxygen defect content in the structure: the slabs  $|\text{Ba}_{1.5}\text{La}_{0.5}\text{Cu}_3\text{O}_7|_\infty$  exhibit, themselves, oxygen defects, which may favour slight displacements of the copper and oxygen atoms along  $\vec{c}$  during oxygen intercalation, between the slabs, without changing the  $c$  parameter.

The oxygen intercalation in the second series,  $\text{La}_{2-x}\text{A}_{1+x}\text{Cu}_2\text{O}_{6-x/2+\delta}$ , depends on the nature of the A ions, calcium or strontium, on the rate of substitution  $x$ , and on the oxygen pressure as shown from table III. It can

TABLE III  
*Crystallographic data and analytical results for the oxides*



Quenched oxides (in air)			Annealed oxides (in O <sub>2</sub> )		
Composition	$\delta$	Cell parameters	Composition	$\delta$	Cell parameters
$\text{La}_2\text{SrCu}_2\text{O}_6$	0	$a = 3.865 \text{ \AA}$ $c = 19.887 \text{ \AA}$	$\text{La}_2\text{SrCu}_2\text{O}_{6.2}$	0.20	$a = 3.865 \text{ \AA}$ $c = 20.065 \text{ \AA}$
$\text{La}_{1.9}\text{Sr}_{1.1}\text{Cu}_2\text{O}_{5.97}$	0.02	$a = 3.863 \text{ \AA}$ $c = 19.963 \text{ \AA}$			b
$\text{La}_{1.86}\text{Sr}_{1.14}\text{Cu}_2\text{O}_{5.97}$	0.04	$a = 3.959 \text{ \AA}$ $c = 19.956 \text{ \AA}$	$\text{La}_{1.86}\text{Sr}_{1.14}\text{Cu}_2\text{O}_{6.22}$	0.29	$a = 3.868 \text{ \AA}$ $c = 20.051 \text{ \AA}$
$\text{La}_{1.9}\text{Ca}_{1.1}\text{Cu}_2\text{O}_{5.97}$	0.02	$a = 3.825 \text{ \AA}$ $c = 19.404 \text{ \AA}$	$\text{La}_{1.9}\text{Ca}_{1.1}\text{Cu}_2\text{O}_{6.02}$	0.08	$a = 3.825 \text{ \AA}$ $c = 19.404 \text{ \AA}$

indeed be seen for the strontium oxides synthesized in air, like  $\text{La}_2\text{SrCu}_2\text{O}_6$ , that  $\delta$  increases with the strontium content tending towards the formulation  $\text{La}_{2-x}\text{A}_{1+x}\text{Cu}_2\text{O}_6$ . It results that the  $\text{Cu}^{3+}$  content increases with the divalent A ion content, in order to compensate the oxygen vacancies due to the substitution of  $\text{Sr}^{2+}$  or  $\text{Ca}^{2+}$  for  $\text{La}^{3+}$ . The annealing of the latter oxides at 400° C under an oxygen pressure of one bar shows the ability of these phases to intercalate oxygen,  $\delta$  ranging from 0 to 0.29 for  $\text{La}_{2-x}\text{Sr}_{1+x}\text{Cu}_2\text{O}_{6-x/2+\delta}$  whereas  $0.02 \leq \delta \leq 0.08$  for  $\text{La}_{1.9}\text{Ca}_{1.1}\text{Cu}_2\text{O}_{5.95+\delta}$ . One can see that the rate of intercalation is higher for the strontium oxides than for the calcium compound. Moreover it seems that in the strontium oxides the maximum rate of intercalation increases with the strontium content. Contrary to the oxides  $\text{La}_3\text{Ba}_3\text{Cu}_6\text{O}_{14+\delta}$ , the compounds  $\text{La}_{2-x}\text{Sr}_{1+x}\text{Cu}_2\text{O}_{6-x/2+\delta}$  exhibit a variation of the interlayer distances: the  $c$  parameter of the tetragonal cell increases with the oxygen content  $\delta$ , for a same  $x$  value. This influence of

intercalation on the  $c$  parameter, can be explained by the fact that the  $|\text{La}_{1-x}\text{Sr}_x\text{Cu}_2\text{O}_6|_\infty$  slabs, which are stoichiometric and formed of SrO-type layers are more rigid than the  $|\text{Ba}_{1.5}\text{La}_{0.5}\text{Cu}_3\text{O}_7|_\infty$  slabs, and are only displaced by the introduction of oxygen between them. However the behaviour of the oxides  $\text{La}_{1.9}\text{Ca}_{1.1}\text{Cu}_2\text{O}_{6-x/2+\delta}$  where  $c$  parameter is independent of  $\delta$  is not explained; nevertheless in this latter case  $\delta$  remains rather weak ( $\delta \leq 0.08$ ). The oxygen desintercalation of these oxides is similar to that observed for the first family: for instance heating the most oxidized compound  $\text{La}_2\text{SrCu}_2\text{O}_{6.20}$  at  $400^\circ\text{C}$  under low oxygen pressures ( $\sim 10^{-3}$  bar) leads progressively to the reduced phase  $\text{La}_2\text{SrCu}_2\text{O}_6$ .

The behaviour of the oxides  $\text{La}_{2-x}\text{A}_x\text{CuO}_{4-x/2+\delta}$  is much more complex owing to the wide homogeneity ranges observed for these oxides especially in the case of strontium. For instance, the  $\delta$  values observed for the strontium oxides synthesized in air (table I) do not increase progressively with  $x$  contrary to  $\text{La}_{2-x}\text{Sr}_{1+x}\text{Cu}_2\text{O}_{6-x/2+\delta}$ , but increase up to  $x \simeq 1/3$  and then decrease again up to  $x \simeq 1$ . These  $\delta$  values are difficult to compare owing to the fact that the different compositions were not synthesized at the same temperature in order to obtain pure oxides. It is sure that equilibrium is rarely reached for this series. So, for  $0 \leq x \leq 1$  the  $\delta$  values given in table I correspond to heating times of 12 h and annealing these samples in the same conditions, but for longer times (24 h to 48 h) allowed us to prepare pure phases with the same structure but characterized by greater  $\delta$  values. Thus it appears that kinetics plays an important part for oxygen intercalation in this phase at a given temperature and a given oxygen pressure. Like for the two other series, oxygen can be intercalated or desintercalated by annealing the samples synthesized in air, at  $400^\circ\text{C}$  under an oxygen pressure of one bar or under vacuum ( $10^{-3}$  bar) respectively. The curves  $\delta = f(x)$  are given in figure 4 for the strontium compounds where they are compared with the line  $\delta = x/2$  which represents the maximum rate of intercalation available in this structure. It can be seen that oxygen can easily be desintercalated, tending towards the most oxygen defect structure; it appears that intercalation tends to be maximum for low  $x$  values ( $0 \leq x \leq 0.25$ ), whereas it is only partial for higher  $x$  values ( $0.33 \leq x \leq 1.20$ ), 11 % to 33 % of the available anionic sites being only occupied in this latter composition range. From these results it seems that intercalation is governed by two opposite effects which are competitive: the trend to preserve a stoichiometric  $\text{K}_2\text{NiF}_4$  structure as for  $\text{La}_2\text{Cu}^{\text{II}}\text{O}_4$  and  $\text{LaSrCu}^{\text{III}}\text{O}_4$  and the trend to form a related defect structure but with an ordering of the oxygen vacancies. Thus, rather close to the stoichiometric compound  $\text{La}_2\text{CuO}_4$  the trend to stoichiometry is favoured by partial oxi-

dition of Cu(II) to Cu(III), whereas rather far from  $\text{La}_2\text{CuO}_4$ , for example for  $x = 1$ , the stoichiometric oxide  $\text{LaSrCuO}_4$  [3] cannot be stabilized any more under normal oxygen pressure, and oxygen vacancies are favoured; the resulting great amount of anionic vacancies are ordered, leading to different microphases as observed by electron diffraction. The «  $a$  » parameter which characterizes the corresponding  $\text{K}_2\text{NiF}_4$  type tetragonal cell is generally not influenced by the intercalation-desintercalation process except for high  $x$  values which exhibit superstructures. For such oxygen defect oxides, an order-disorder phenomenon of the oxygen vacancies appears in the (0 0 1) plane which contributes to the variation of the «  $a$  » parameter of the  $\text{K}_2\text{NiF}_4$  subcell. It is for instance the case of the strontium oxide corresponding to  $x = 1.20$ . The sample quenched in air ( $\delta = 0$ ) exhibits a superstructure in the (0 0 1) plane with a «  $a$  » subcell parameter of 3.76 Å (table I). The annealing at 400° C in oxygen of this phase involves an important decrease of the rate of the oxygen vacancies ( $\delta = 0.33$ ). It results that the order disappears, leading to a true tetragonal cell with «  $a$  » greater than that of the quenched specimen ( $a = 3.791$  Å),  $c$  being smaller ( $c = 12.900$  Å). The evolution of the  $c$  parameter versus composition for quenched and annealed compounds is complex (fig. 5). It results from the influence of several factors: copper (III) and oxygen vacancies contents, size of  $\text{Sr}^{2+}$  which is slightly larger than  $\text{La}^{3+}$ . For every  $x$  value,  $c$  increases with the rate of intercalation, *i. e.* with the  $\text{Cu}^{3+}/\text{Cu}^{2+}$  ratio, except for high  $x$  values which exhibit order-disorder phenomena. This behavior is in agreement with the observation previously made by Goodenough *et al.* [3].

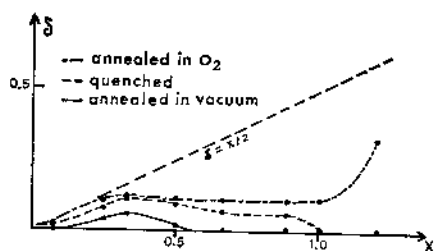


Fig. 4.

Fig. 4. — The oxides  $\text{La}_{2-x}\text{Sr}_x\text{CuO}_{4-x/2+\delta}$ : evolution of  $\delta$  as a function of  $x$  for oxides resulting from different thermal treatments.

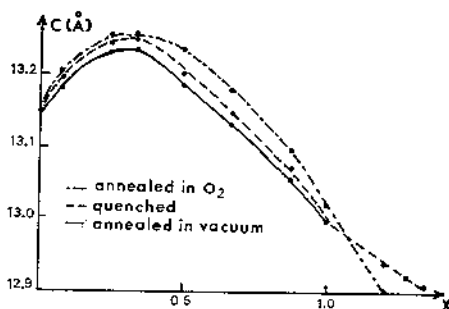


Fig. 5.

Fig. 5. — The oxides  $\text{La}_{2-x}\text{Sr}_x\text{CuO}_{4-x/2+\delta}$ : evolution of the  $c$  parameter as a function of  $x$  for oxides resulting from different thermal treatments.

The evolution of «  $c$  » can be interpreted by two opposite effects: increasing due to substitution of  $\text{Sr}^{2+}$  for  $\text{La}^{3+}$  and decreasing due to oxygen vacancies. For small  $x$  values ( $x < 0.25$ ) the number of oxygen vacancies remains low and tends towards zero so that  $c$  increases owing to the replacement of  $\text{La}^{3+}$  by  $\text{Sr}^{2+}$ . For  $x > 0.25$  the number of oxygen vacancies becomes very large and its effects prevails on that of substitution  $\text{Sr}^{2+}/\text{La}^{3+}$ , involving a decrease of «  $c$  ».

### INFLUENCE OF THE INTERCALATION PROCESS ON THE ELECTRICAL PROPERTIES OF THE MIXED VALENCE COPPER OXIDES

Most of the oxides described above are characterized by the presence simultaneously of Cu(II) and Cu(III), and are thus mixed-valence oxides. The electron transport properties of these phases, which are  $p$  type semiconductors or  $p$  type semi-metals or metals are strongly influenced by the rate of intercalation.

The evolution of conductivity versus reciprocal temperature for different

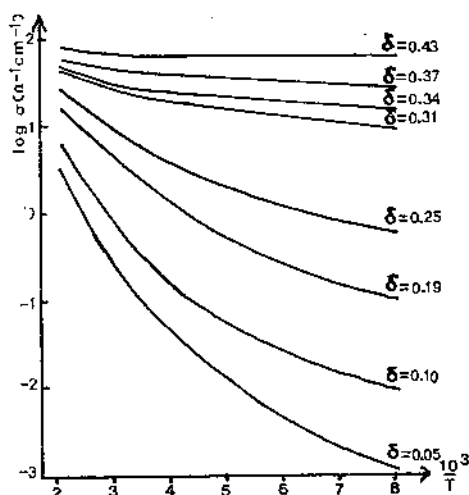


Fig. 6.

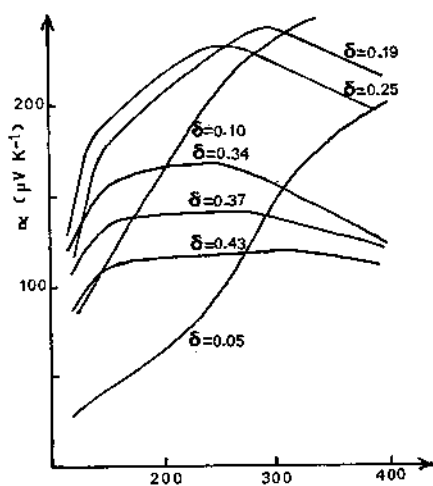


Fig. 7.

Fig. 6. — The oxides  $\text{Ba}_3\text{La}_3\text{Cu}_6\text{O}_{14+\delta}$ : variation of the conductivity (logarithmic scale) as a function of reciprocal temperature for different  $\delta$  values.

Fig. 7. — The oxides  $\text{Ba}_3\text{La}_3\text{Cu}_6\text{O}_{14+\delta}$ : variation of the thermoelectric power as a function of  $T$  for different  $\delta$  values.

$\delta$  values of the oxides  $\text{La}_3\text{Ba}_3\text{Cu}_6\text{O}_{14+\delta}$  (fig. 6) shows that the conductivity increases drastically with the intercalation of oxygen, contrary to the structure which remains unchanged. In the same way the thermoelectric power of these phases (fig. 7) is very sensitive to the intercalation rate. These properties are interpreted by a conduction band model whose configuration is mainly determined by the splitting of the  $3d$  Cu orbitals by the crystal field [15] (fig. 8 a). Every composition can indeed be considered as a mixing of the two limits: the reduced form  $\text{Ba}_3\text{La}_3\text{Cu}_6\text{O}_{14}$  characterized by ribbons of one octahedron and two tetragonal pyramids running along  $\vec{c}$ , and the oxidized form  $\text{Ba}_3\text{La}_3\text{Cu}_6\text{O}_{15}$  which exhibits infinite octahedral ribbons along  $\vec{c}$ . The  $\sigma_{x^2-y^2}$  bands result from Cu - O - Cu interactions and strong electron-electron interactions split the  $dz_{1/2}^2$  and  $dz_{2/2}^2$  levels by a few eV like the  $\sigma_{x^2-y^2}^{*1}$  and  $\sigma_{x^2-y^2}^{*2}$  bands. It results that the band structure of  $\text{La}_3\text{Ba}_3\text{Cu}_6\text{O}_{14}$  (fig. 8 b) is that of an insulator but this limit has not been synthesized; on the other hand, the only level configuration which can lead to a semi-metallic or metallic conduction for the limit  $\text{Ba}_3\text{La}_3\text{Cu}_6\text{O}_{15}$  corresponds to a  $dz_{1/2}^2$  empty level located just above or across the filled

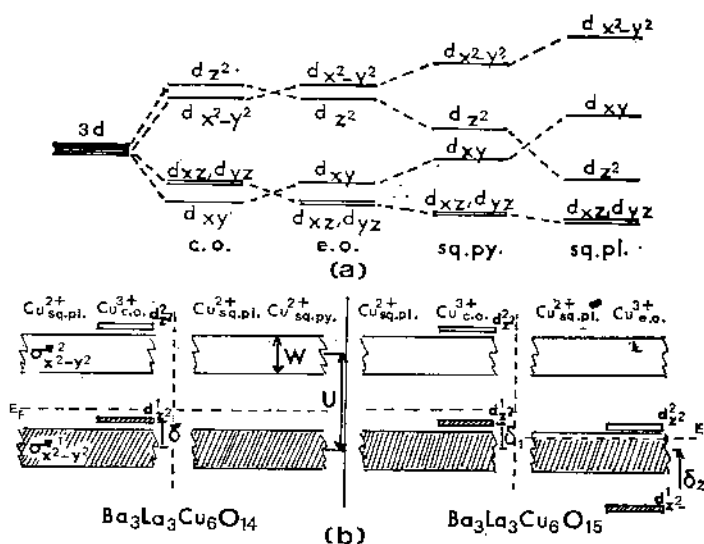


Fig. 8.

- a) Crystal field splitting for  $d$  element in different environments; c. o.: compressed octahedron, e. o.: elongated octahedron, sq. py.: square pyramid, sq. pl. square plane.  
 b) Schematic band diagram for  $\text{Ba}_3\text{La}_3\text{Cu}_6\text{O}_{14}$  and  $\text{Ba}_3\text{La}_3\text{Cu}_6\text{O}_{15}$ .  $U$  denotes the intra-atomic coulomb energy,  $\delta$ ,  $\delta_1$  and  $\delta_2$  the splitting due to the axial distortion of the octahedra and  $W$  the estimated band width.

$\sigma_{x^2-y^2}^{*1}$  band (fig. 8 b). Thus, it appears that intercalation of oxygen which corresponds to a local change of copper coordination, will involve an increase of the density of the  $dz_{x^2-y^2}^2$  levels above the filled  $\sigma_{x^2-y^2}^{*1}$  band, *i. e.* an increase of the number of holes in the conduction band. The approximately linear evolution of  $\log \sigma$  vs  $\delta$  at 293 K is in agreement with this model. This progressive transition from a semi-conductive to a semi-metallic state can be explained by the Mott model [16] of quasi localized holes trapped at the top of the filled  $3d_{x^2-y^2}$  band.

The oxides  $\text{La}_{2-x}\text{A}_{1+x}\text{Cu}_2\text{O}_{6-x/2+\delta}$  exhibit a similar behaviour [17]. From the evolution of the curves  $\log \sigma = f(1/T)$ , between 80 K and 300 K (fig. 9) it can be seen that a continuous transition from a semi-conductive to a semi-metallic state is observed as the oxygen intercalation rate increases from  $\delta = 0$  ( $\text{La}_2\text{SrCu}_2\text{O}_6$ ) to  $\delta = 0.29$  ( $\text{La}_{1.86}\text{Sr}_{1.14}\text{Cu}_2\text{O}_{6.22}$ ). The conductivity depends also on the nature of the A ion which influences drastically the  $c$  parameter: the calcium oxide  $\text{La}_{1.90}\text{Ca}_{1.10}\text{Cu}_2\text{O}_{5.97}$  is indeed much more conductor than the corresponding strontium oxide  $\text{La}_{1.90}\text{Sr}_{1.10}\text{Cu}_2\text{O}_{5.97}$ . The Seebeck coefficient curves  $\alpha = f(T)$  (fig. 10) confirm this influence of intercalation:  $\alpha$  increases continuously with T for

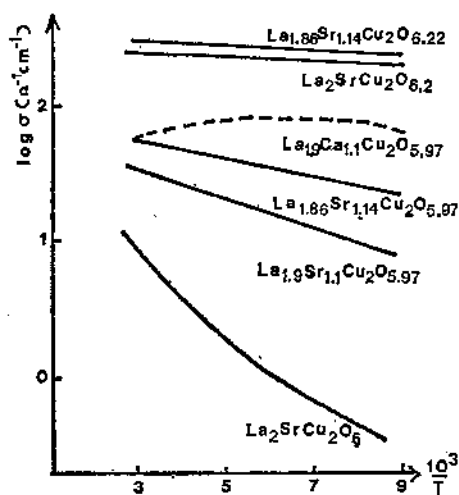


Fig. 9.

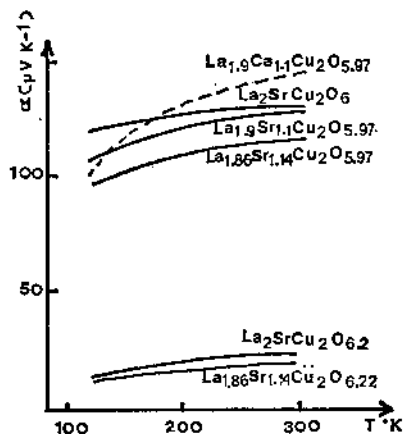


Fig. 10.

Fig. 9. — The oxides  $\text{La}_{2-x}\text{A}_{1+x}\text{Cu}_2\text{O}_{6-x/2+\delta}$ : evolution of the conductivity (logarithmic scale) vs  $T^{-1}$  for different compositions.

Fig. 10. — The oxides  $\text{La}_{2-x}\text{A}_{1+x}\text{Cu}_2\text{O}_{6-x/2+\delta}$ : evolution of the thermoelectric power vs T for different compositions.

the small intercalation rates ( $\delta = 0$  to 0.04) *i. e.* for small  $\text{Cu}^{3+}$  contents, whereas it becomes weak and nearly independent of the temperature, for high intercalation rates ( $\sigma = 0.20$  to 0.29), *i. e.* for high hole concentration. These properties very similar to those obtained for  $\text{La}_3\text{Ba}_3\text{Cu}_6\text{O}_{14+\delta}$  can be explained by the same Mott model of holes trapped at the top of the  $\sigma_{x^2-y^2}^{*1}$  band. However the rather high conductivity of  $\text{La}_2\text{SrCu}_2\text{O}_6$  in spite of the very weak  $\text{Cu}^{3+}$  content— $\delta \simeq 0$ —let us think that the intra-atomic energy  $U$  is in this case of the same order of magnitude as the band width  $W_\sigma$  (fig. 11). In the same manner the relatively high and metallic conductivity of the calcium oxide  $\text{La}_{1.90}\text{Ca}_{0.10}\text{Cu}_2\text{O}_{5.97}$  compared to the corresponding strontium oxide shows that the band width  $W_\sigma$  must be larger than  $U$  in the calcium compound so that the overlapping of the two  $\sigma_{x^2-y^2}^{*}$  bands gives rise to a higher mobility.

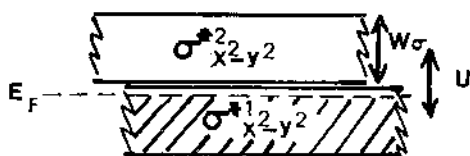


Fig. 11. — The oxides  $\text{La}_{2-x}\text{A}_{1+x}\text{Cu}_2\text{O}_{6-x/2+\delta}$ : schematic band diagram as deduced from electron transport properties.

The highest conductivities are observed for the oxides  $\text{La}_{2-x}\text{Sr}_x\text{CuO}_{4-x/2+\delta}$  [18]. For a given substitution rate  $x$ , the conductivity increases with the rate of intercalation  $\delta$  as shown from figure 12 for temperature ranging from 80 K to 300 K. However the evolution of  $\log \sigma$  vs  $1/T$  as well as  $\alpha = f(T)$  is more complex than the two other series:  $\delta$  is not the only factor governing the electron transport properties of the phases. Three domains must in fact be distinguished:  $0 \leq x \leq 0.16$ ,  $0.16 < x \leq 0.50$  and  $0.50 < x \leq 1.20$  for the oxides quenched in air and annealed in oxygen. The compounds of the first domain ( $0 \leq x \leq 0.16$ ) are characterized by a semi-metallic behaviour and their properties can be interpreted by the model developed by Goodenough for  $\text{La}_2\text{CuO}_4$  [19] involving the presence of holes in the filled band  $\sigma_{x^2-y^2}^{*1}$ . The weak variation of conductivity which does not correspond to the metallic model  $\rho = \rho_0(1 + \gamma t)$  (fig. 12 a), as well as the thermoelectric power values (fig. 13) greater than those of a metal are in agreement with this model. The fact that the holes may be trapped on localized levels at the top of the  $\sigma_{x^2-y^2}^{*1}$  band according to the Mott Model is also confirmed by the fact that  $\alpha$  increases with temperature (fig. 13). The

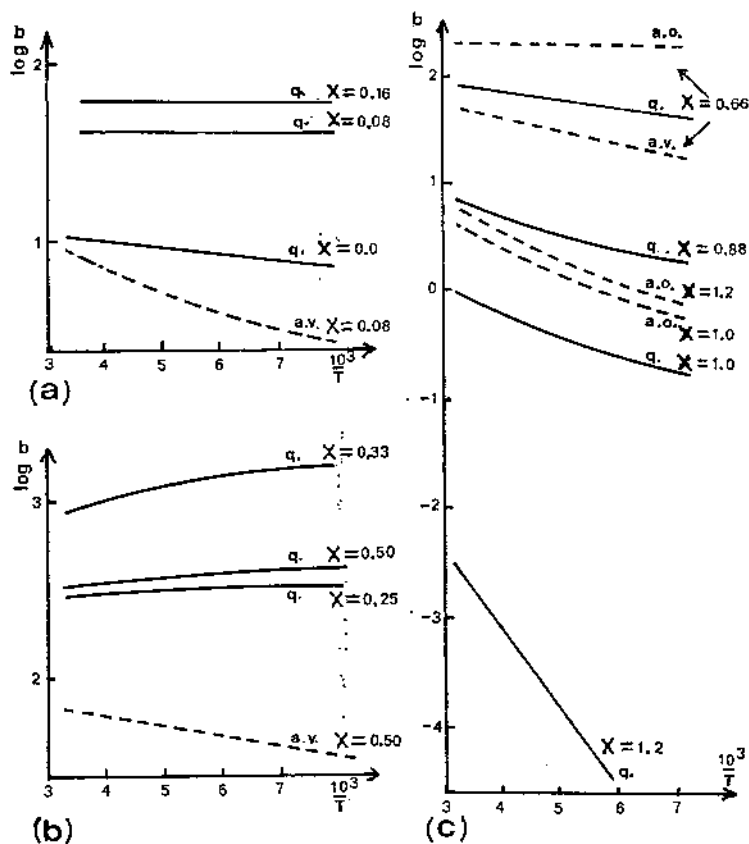


Fig. 12. — The oxides  $\text{La}_{2-x}\text{Sr}_x\text{CuO}_{4-x/2+\delta}$ : variation of the conductivity vs  $T^{-1}$  (q: quenched in air, a. o.: annealed in  $\text{O}_2$ , a. v.: annealed in vacuum).

a)  $0 \leq x \leq 0.16$ ; b)  $0.16 < x \leq 0.50$ ; c)  $0.5 < x \leq 1.20$ .

oxides belonging to the second domain ( $0.16 < x \leq 0.50$ ), exhibit a metallic conductivity (fig. 12 b) which increases with the intercalation rate:  $\rho$  increases linearly with temperature and the thermoelectric power values are weak and nearly temperature independent (fig. 13). The highest  $x$  compositions ( $0.50 < x \leq 1.20$ ), exhibit for the less oxidized compounds synthesized in air ( $\delta < 0.07$ ) a semi-conductive behaviour:  $\sigma$  decreases drastically with  $\delta$  (fig. 12 c), and correlatively  $\alpha$  increases as  $\delta$  decreases (fig. 13). These latter oxides and especially the compositions corresponding to  $x = 0.88$ , 1 and 1.2 exhibit a variation of the conductivity according to the Mott' relation  $\sigma = A \exp [-(Q/k_0T)^{1/4}]$  which characterizes a variable range hopp-

ing of holes located in the  $\sigma_{x^*1-y_2}$  band close to the Fermi level. It must be noted that the electrical properties of the oxides  $\text{La}_{2-x}\text{Sr}_x\text{CuO}_{4-x/2+\delta}$  do not depend on the  $\delta$  value only. So, for instance, the oxides corresponding to  $0.33 \leq x \leq 1.0$  which have been annealed under an oxygen pressure of 1 bar exhibit the same  $\delta$  value ( $\delta \simeq 0.11$ ), but are characterized by a decrease

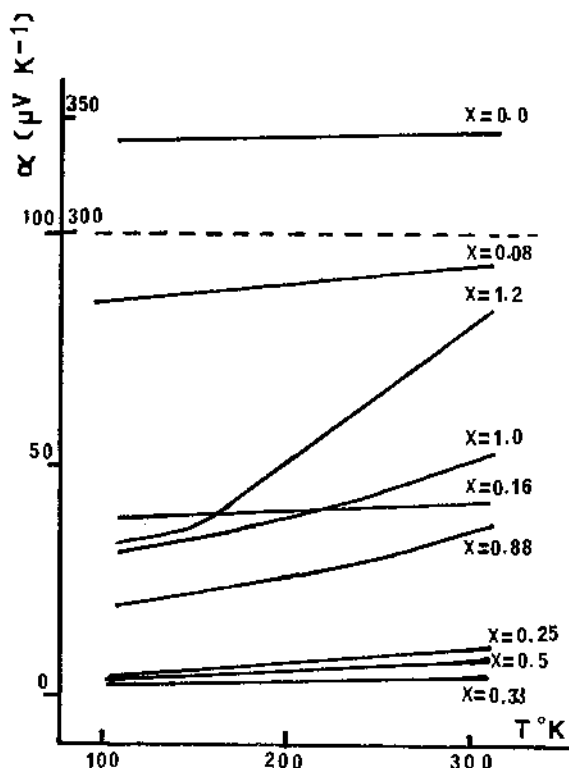


Fig. 13. — The oxides  $\text{La}_{2-x}\text{Sr}_x\text{CuO}_{4-x/2+\delta}$ : thermoelectric power vs T for quenched oxides with different x values.

of  $\sigma$  as  $x$  increases as shown figure 14. This shows the influence of the rate of anionic vacancies ( $x/2-\delta$ ) on the carrier mobility. Moreover the distribution of the oxygen defects *i. e.*; the order-disorder phenomena, may influence the electron transport properties of these compounds.

The great sensitivity of these compounds to oxygen makes that their electrical conductivity can vary drastically, under a given oxygen pressure owing to the intercalation or deintercalation of oxygen. For this reason

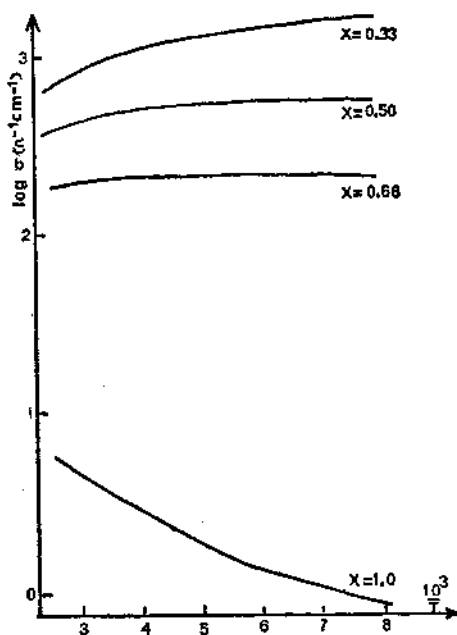


Fig. 14. — The oxides  $\text{La}_{2-x}\text{Sr}_x\text{CuO}_{4-x/2+\delta}$ : evolution of the conductivity as a function of reciprocal temperature for oxides annealed under an oxygen pressure of 1 bar ( $\delta \approx 0.11$ ,  $0.33 \leq x \leq 1.0$ ).

we have only discussed above the electrical properties of these phases at relatively low temperatures ( $T < 300$  K), where all the compounds of the three families are not sensitive to intercalation or desintercalation. Such anomalies of the conductivity have indeed been observed for the oxides  $\text{La}_{2-x}\text{Sr}_x\text{CuO}_{4-x/2+\delta}$  corresponding to  $0 \leq x \leq 0.16$  and synthesized in air ( $0 \leq \delta \leq 0.04$ ). One indeed observes (fig. 15), beyond 300 K under an oxygen pressure of 0.2 bar that  $\sigma$  decreases first drastically in the temperature range 300 K-420 K and then increases again in the temperature range 420 K-650 K. The thermogravimetric curves of these phases, characterized successively by a weight loss and weight gain, show clearly that this behaviour results from desintercalation and intercalation of oxygen successively. Similar properties are observed for the oxides  $\text{La}_{2-x}\text{Sr}_{1+x}\text{Cu}_2\text{O}_{6-x/2+\delta}$  synthesized in air for  $x = 0.1$  and 0.14 (fig. 15) and for which the thermogravimetric measurements confirm the oxygen desintercalation-intercalation process. The reversibility of the intercalation process in these phases is illustrated by the evolution of the conductivity of  $\text{La}_{1.9}\text{Ca}_{1.1}\text{Cu}_2\text{O}_{5.97}$  versus reciprocal

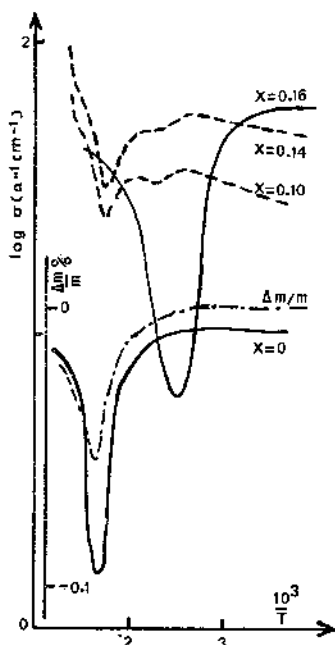


Fig. 15.

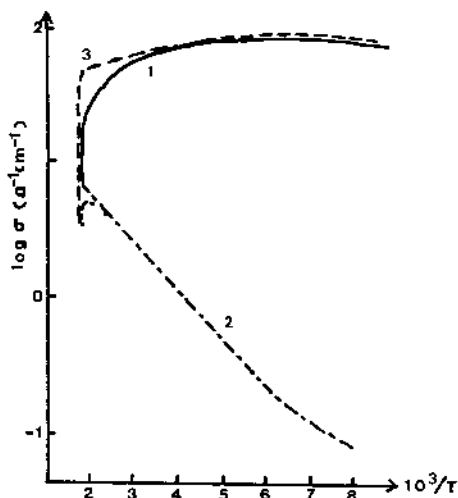


Fig. 16.

Fig. 15. — Variation of conductivity vs  $T^{-1}$  ( $T > 300\text{K}$ ) in air for some oxides in the  $\text{La}_{2-x}\text{Sr}_x\text{CuO}_{4-x/2+\delta}$  series (solid line) and in the  $\text{La}_{2-x}\text{Sr}_{1+x}\text{Cu}_2\text{O}_{6-x/2+\delta}$  series (dotted line). A TG curve for  $x = 0$  (first series), with the same temperature scale is given as example to illustrate the close relation between variation of conductivity and oxygen amount.

Fig. 16. — Variation of conductivity vs  $T^{-1}$  for the oxides  $\text{La}_{1.3}\text{Ca}_{1.1}\text{Cu}_2\text{O}_{6.9}$ ; under different atmospheres:

- 1) — first heating under inert atmosphere,
- 2) - - - first cooling and second heating under inert atmosphere,
- 3) - - - air introduction and second cooling (in air).

temperature under argon and air (fig. 16). The behaviour of this phase is indeed very different in argon and in air. The conductivity decreases under argon as soon as the temperature is greater than 300 K, owing to the departure of oxygen and at about 570 K  $\sigma$  decreases drastically. At this stage of the experiment, heating is stopped and the sample is cooled progressively down to 77 K. In this latter temperature range a semi-conductive behaviour is observed owing to the lower oxygen rate of intercalation. Heating again up to 500 K under argon leads to the same curve. However

beyond 500 K,  $\sigma$  decreases again; this phenomenon is due to the fact that the thermodynamical equilibrium is not yet reached when we stop heating at 570 K. At 570 K argon is replaced by air, and heating is stopped. It can be seen that the conductivity increases immediately owing to the oxygen intercalation. The behaviour observed from 570 K to 77 K is then similar to that observed for the starting material.

## REFERENCES

- [1] J. M. LONGO, P. M. RACCAH, *J. Solid State Chem.*, 1973, **6**, p. 526.
- [2] S. GRANDE, H. MÜLLER-BUSCHAUM, M. SCHWEITZER, *Z. Anorg. Allg. Chem.*, 1977, **428**, p. 120.
- [3] J. B. GOODENOUGH, G. DEMAZEAU, M. POUCHARD, P. HAGENMÜLLER, *J. Solid State Chem.*, 1973, **8**, p. 325.
- [4] W. KLEMM, G. WEHRMAYER, H. BADE, *Elektrochem. Ber. Bunsenges Phys. Chem.*, 1959, **63**, p. 56.
- [5] K. HESTERMANN, R. HOPPE, *Z. Anorg. Allg. Chem.*, 1969, **367**, p. 249.
- [6] K. HESTERMANN, R. HOPPE, *Z. Anorg. Allg. Chem.*, 1969, **367**, p. 261.
- [7] K. HESTERMANN, R. HOPPE, *Z. Anorg. Allg. Chem.*, 1969, **367**, p. 270.
- [8] G. DEMAZEAU, C. PARENT, M. POUCHARD, P. HAGENMÜLLER, *Mat. Res. Bull.*, 1972, **7**, p. 913.
- [9] M. ARJOMAND, D. MACHIN, *J. Chem. Soc. Dalton Trans.*, 1975, p. 1061.
- [10] H. N. MIGEON, F. JEANNOT, M. ZANNE, J. AUBRY, *Rev. Chim. Miner.*, 1976, **13**, p. 440.
- [11] N. NGUYEN, L. ER-RAKHO, C. MICHEL, J. CHOISNET, B. RAVEAU, *Mat. Res. Bull.*, 1980, **15**, p. 891.
- [12] L. ER-RAKHO, C. MICHEL, J. PROVOST, B. RAVEAU, *J. Solid State Chem.*, 1981, **37**, p. 151.
- [13] N. NGUYEN, J. CHOISNET, M. HERVIEU, B. RAVEAU, *J. Solid State Chem.*, 1981, **39**, p. 120.
- [14] J. PROVOST, F. STUDER, C. MICHEL, B. RAVEAU, *Synthetic Metals*, 1981, **4**, p. 147.
- [15] J. PROVOST, F. STUDER, C. MICHEL, B. RAVEAU, *Synthetic Metals*, 1981, **4**, 157.
- [16] N. F. MOTT, *Metal-Insulator Transitions*, Taylor and Francis, London, 1974.
- [17] N. NGUYEN, C. MICHEL, F. STUDER, B. RAVEAU, *Mat. Chem.*, 1982, **7**, p. 413.
- [18] N. NGUYEN, F. STUDER, B. RAVEAU, *J. Phys. Chem. Solids*, 1983, **44**, p. 389.
- [19] J. B. GOODENOUGH, *Mat. Res. Bull.*, 1973, **8**, p. 423.

(Received December 12, 1983)